Article:
Li, J, Li, S, Zheng, Y et al. (9 more authors) (2019) Fast preparation of rhamnogalacturonan I enriched low molecular weight pectic polysaccharide by ultrasonically accelerated metal-free Fenton reaction. Food Hydrocolloids, 95. pp. 551-561. ISSN 0268-005X

https://doi.org/10.1016/j.foodhyd.2018.05.025

Accepted Manuscript

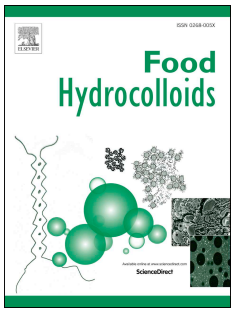

ssFast preparation of rhamnogalacturonan I enriched low molecular weight pectic polysaccharide by ultrasonically accelerated metal-free Fenton reaction

Junhui Li, Shan Li, Yangfan Zheng, Hua Zhang, Jianle Chen, Lufeng Yan, Tian Ding, Robert J. Linhardt, Caroline Orfila, Donghong Liu, Xingqian Ye, Shiguo Chen

PII: S0268-005X(18)30380-1

DOI: 10.1016/j.foodhyd.2018.05.025

Reference: FOOHYD 4443

To appear in: *Food Hydrocolloids*

Received Date: 2 March 2018

Revised Date: 11 May 2018

Accepted Date: 12 May 2018

Please cite this article as: Li, J., Li, S., Zheng, Y., Zhang, H., Chen, J., Yan, L., Ding, T., Linhardt, R.J., Orfila, C., Liu, D., Ye, X., Chen, S., ssFast preparation of rhamnogalacturonan I enriched low molecular weight pectic polysaccharide by ultrasonically accelerated metal-free Fenton reaction, *Food Hydrocolloids* (2018), doi: 10.1016/j.foodhyd.2018.05.025.

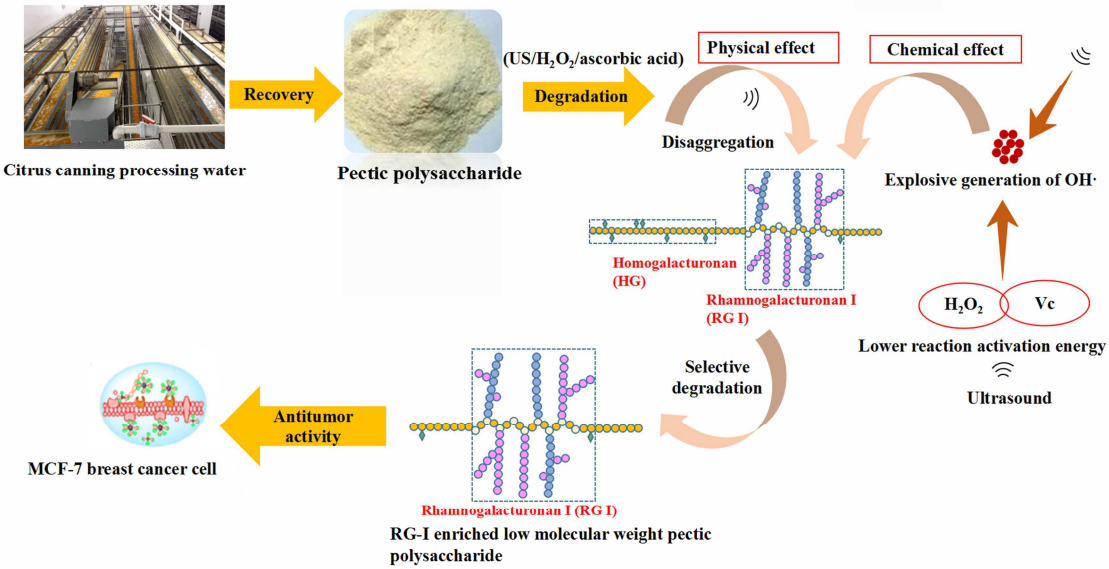

ssFast preparation of rhamnogalacturonan I enriched low molecular weight pectic polysaccharide by ultrasonically accelerated metal-free Fenton reaction

Junhui Li[1], Shan Li[1], Yangfan Zheng[1], Hua Zhang[1], Jianle Chen[1], Lufeng Yan[1], Tian Ding[1], Robert J. Linhardt [2], Caroline Orfila[3], Donghong Liu[1], Xingqian Ye[1], Shiguo Chen*[1]

1. Zhejiang Key Laboratory for Agro-Food Processing, Department of Food Science and Nutrition, Fuli Institute of Food Science, Zhejiang University, Hangzhou 310058, China.

2. Center for Biotechnology & Interdisciplinary Studies, Department of Chemistry & Chemical Biology, Rensselaer Polytechnic Institute, Biotechnology Center 4005, Troy, NY 12180, USA.

3. School of Food Science and Nutrition, University of Leeds, Leeds LS2 9JT, UK.

* Correspondence: College of Biosystem Engineering and Food Science, Zhejiang University, Hangzhou 310029, China, chenshiguo210@163.com; Tel/Fax: +86-0571-8898-2151

Abstract

The recovery of pectic polysaccharides with high rhamnogalacturonan I (RG-I) branches from citrus canning processing water was achieved in a previous study aimed at reducing chemical oxygen demand and benefiting both process economics and the environment. However, the large molecular size and poor *in vivo* bioavailability of these polysaccharides limit the application of these pectic polysaccharides in functional foods. We report the development of an ultrafast and green approach to depolymerize pectic polysaccharides using an ultrasound-accelerated metal-free Fenton chemistry, relying on H_2O_2/ascorbic acid. The results show that ultrasound enhances the efficiency of H_2O_2/ascorbic acid system to degrade pectin into 7.9 kDa pectic fragments within 30 min through both chemical effects (increasing the amount of hydroxyl radicals and lowering activation energy of H_2O_2 decomposition) and mechanical effects (disaggregating polysaccharide clusters). The backbones of the resulting fragments mainly correspond to RG-I patterns (molar ratio galacturonic acid (GalA): rhamnose (Rha) ~ 1.06:1) with a high degree of rhamnose branching. Free radicals preferentially act on the GalA backbone in the HG region and maintain the RG-I region. Antitumor activities, assessed using human breast cancer cells (MCF-7), suggest that the resulting fragments significantly inhibit cancer cell growth and that activity increases with decreasing molecular weight. The resulting ultralow molecular weight pectic fragments have potential application for the development of functional foods and antitumor drugs.

Key words: citrus canning water; pectic polysaccharide; non-metal Fenton chemistry; ultrafast green degradation; antitumor activity

1. Introduction

Canned citrus segments occupy an important sector of the world's fruit production, with an annual trade value of nearly $900 million (source: UN Comtrade). As the largest citrus planting and harvesting country in the world, China accounts for near 70% canned citrus segments on the international market (Wu et al., 2016). However, the industry produces about one million pounds of solid and liquid waste (principally polysaccharides) with high chemical oxygen demand (COD) (~10,000 mg/L) every year, representing both an economic and an environmental challenge (Chen et al., 2017). The organic substances present in the processing water mainly consist of pectic polysaccharides (PPs) (Chen et al., 2017) and these polysaccharides have potential use in food industry as thickeners and gelling agents.

In our previous study, we recovered PPs from basic water during the segment membrane removal process, taking place in citrus canning factories. These PPs were dominated by rhamnogalacturonan I regions with almost no esterification (Chen et al., 2017). RG-I enriched PPs, in dietary sources, are known to demonstrate a broad range of pharmacologic properties, such as antitumor (Zhi et al., 2017), prebiotic (Karboune & Khodaei, 2016), and immunomodulatory activities (Dikeman & Fahey, 2006). Despite multiple biomedical uses, these PPs have high molecular weights and, thus, show poor solubility and marginal bioavailability (Moreno, 2014). Recent research has demonstrated that low-molecular-weight pectin polysaccharides (LMPs) have improved bioavailability

64 (Kapoor & Dharmesh, 2017), greater prebiotic potential (Belén Gómez, 2016) and higher
65 immune-modulating (Shin, Kiyohara, Matsumoto, & Yamada, 1997; Matsumoto, Moriya,
66 Sakurai, Kiyohara, Tabuchi, & Yamada, 2008; Matsumoto, Guo, Ikejima, & Yamada,
67 2003), anti-ulcer and anti-inflammatory activities. Therefore, the preparation of LMPs is
68 currently of great interest. However, to the best of our knowledge, the preparation of
69 LMPs from citrus canning processing water has not been reported.

70 Controlled chemical depolymerization processes, mainly relying on acid or enzymatic
71 treatment (Khodaei & Karboune, 2016; Khotimchenko, 2012; Leclere, Cutsem, &
72 Michiels, 2013; Hao, 2013) and physical treatments, such as ultrasound (Zhang et al.,
73 2013), heat (Leclere, Cutsem, & Michiels, 2013; Ramos-Aguilar et al., 2015), high
74 pressure microfluidization (Chen et al., 2013) and gamma-irradiation (Dogan, Kayacier, &
75 Ic, 2007) have been used to prepare LMPs. The conditions for acid-catalyzed hydrolysis
76 are usually fairly drastic, leading to the cleavage of different glycosidic linkages with low
77 selectivity, and results in a variety of different LMP preparations (Garna, Mabon, Wathelet,
78 & Paquot, 2004). Enzymatic hydrolysis of pectin is more selective, but requires the use of
79 different types of enzymes, increasing the costs of the depolymerization process. In
80 addition, during hydrolysis, potential microbial contamination of LMP preparations can
81 result in decreased yields and lead to the formation of unwanted byproducts, further
82 limiting its broad industrial application (Grohmann, Cameron, & Buslig, 1995). Among all
83 the physical treatments reported, ultrasound is considered one of the most effective of the

84 “green” techniques (Ma et al., 2016) used to depolymerize diverse forms of
85 polysaccharides (Zhang et al., 2013). However, the reduction of polysaccharide molecular
86 weight using ultrasound is typically limited to 20 kDa due to the attenuation of energy
87 transmission under prolonged or high-intensity ultrasonic fields (Sun, Ma, Ye, Kakuda, &
88 Meng, 2010).

89 A combination of a Fenton process with ultrasound can significantly improve
90 degradation efficiency, as demonstrated in the pectin depolymerization process (Zhi, et al.,
91 2017). However, strictly acidic conditions (pH < 4) are required in practical applications
92 (Garrido-Ramirez, Theng, & Mora, 2010) and acidic conditions can also lead to the
93 hydrolysis of side-chains and the hydrolysis of the acid-labile linkages between the GalA
94 and Rha residues in the RG-I region (Khalikov & Mukhiddinov, 2004; Levigne, Ralet, &
95 Thibault, 2002). Such acid-catalyzed hydrolysis can significantly impact both bioactivity
96 (Li, Li, & Gao, 2014) and gel forming properties.

97 Non-metal Fenton chemistry is emerging as an alternative technology for the efficient
98 degradation of chemically stable, organic substrates. These systems operate at
99 near-ambient temperatures and pressures and also generate strongly oxidizing radical
100 species (primarily HO•). The key non-metal Fenton-like chemistries include
101 H_2O_2/ascorbic acid and H_2O_2/ozone (O_3). Although the H_2O_2/ozone (O_3) system can also
102 degrade organic substrates with high efficiency, the high cost of O_3 and its toxicity in
103 humans precludes its use. In comparison, the cost of H_2O_2/ascorbic acid system is much

lower and these reagents are currently used within the food industry. The polysaccharide degradation efficiency, using a H_2O_2/ascorbic acid system, is comparable to that of metal catalyzed Fenton system (Verma, Baldrian, & Nerud, 2003). In addition, the H_2O_2/ascorbic acid system is eco-friendly and these reagents are easy to remove, can work in the absence of trace metal and can act over a broad pH range. In our previous study, we demonstrated that ultrasound enhances the efficiency of the metal-catalyzed Fenton reaction in degrading PPs and we elucidated the relevant mechanism (Zhi et al., 2017). However, it is still unclear whether ultrasound can accelerate the polysaccharide degradation efficiency of the non-metal Fenton chemistry.

The present study establishes ultrasound-accelerated non-metal Fenton-like chemistry (H_2O_2/ascorbic acid) to depolymerize PPs from citrus canning processing water, with aim of improving degradation efficiency. A mechanism is proposed for the efficient degradation of PPs by non-metal Fenton-like chemistry. The influence of ascorbic acid concentration, the sonolysis intensities, the reaction temperature, and the combined effect of sonolysis with H_2O_2/ascorbic acid redox system on the molecular weight were determined. The structural properties of the resulting LMPs were characterized by Fourier transform-infrared (FT-IR), nuclear magnetic resonance (NMR) spectroscopy and monosaccharide composition analysis. In addition, the *in vitro* tumor cell growth inhibitory effects and cytotoxicity of PPs and LMPs, were evaluated on MCF-7 human breast

adenocarcinoma cells using 3-(4,5-dimethylthiazol-2-yl)-2,5-diphenyltetrazolium bromide (MTT) assay and lactate dehydrogenase (LDH) assay.

2. Materials and Methods

2.1. Materials.

The basic water discharged from citrus canning factories during the segment membrane removal process, was collected from citrus fruit canning factories (Ningbo, China). Gel-filtration column Ultrahydrogel 250 and TSK-Gel G 4000 SWXL column was from Waters and Tosoh Biosep, respectively. Hydrogen peroxide, ascorbic acid, HPLC-grade methyl alcohol and deuterium oxide were obtained from Sinopharm Chemical Reagent Co., Ltd. (Shanghai, China). The 95% (v/v) ethanol (food grade) and other chemical reagent were acquired from Aladdin Chemical Reagent Co., Ltd. (Shanghai, China).

2.2. Pectic polysaccharide recovery.

Pectic polysaccharide was prepared following a previously reported method (Ye, 2017). Polysaccharide recovery initially involves a two-step filtration process with 200 and 400 meshes filters (size: $\Phi \times h = 1\ m \times 2\ m$) used to eliminate the suspended solid particles. The filtrate is then pumped (13 m^3/h, 11 kW) to the pH adjustment reactor (volume: 8 m^3, stirring power: 4 kW) for neutralization, followed by vacuum concentration (size: 5 m × 6 m × 9 m, 40 kW) at 70 °C. Precipitation (volume: 4 m^3, stirring power: 2

kW) with ethanol at a final ethanol concentration of 50 vol % was performed with gentle stirring. After standing for 30 min, the precipitation was completed and a screw machine (size: 3 m × 0.6 m × 2 m, 0.75 kW) was applied to recover the precipitates, which were the polysaccharides (insoluble in ethanol solution), and the filtrate was then transported to the alcohol recovery unit (integrated with the concentration unit, 12 kW). The precipitate was washed once with 95% ethanol and again ethanol recovered. Subsequently, vacuum drying (size: 1.5 m × 1.5 m × 1.7 m, 5 kW) was conducted on the precipitate (also with ethanol recovery). The dry polysaccharide was ground into a powder to obtain PPs.

2.3. Synergistic effect of ultrasonolysis and H_2O_2/ascorbic acid for depolymerization of pectic polysaccharide.

Ultrasound treatments were performed (Scientz-IID, Ningbo Scientz Biotechnology Co., Ningbo, China) with the following parameters: maximum ultrasound power output, 900 W, frequency, 22 kHz, intermittent type, 2 s on and 2 s off, and horn micro tip diameter, 10 mm. Twenty-five milliliters of PPs solution (5 mg/mL) were placed in a cylindrical glass reactor (Φ, 2.90 cm) and the generator probe was submerged (about 1 cm below the liquid surface) to release ultrasonic energy.

Under the selected conditions, ultrasound/ H_2O_2/ascorbic acid (ultrasonic intensity, 3.8 W/mL, the concentration of ascorbic acid, 10 mM and the concentration of H_2O_2, 50 mM), the results were compared with: single ultrasound treatments (3.8 W/mL),

ultrasound (ultrasonic intensity, 3.8 W/mL) assisted with H_2O_2 (50 mM), ultrasound (ultrasonic intensity, 3.8 W/mL) assisted with ascorbic acid (10 mM), single H_2O_2 (50 mM), single ascorbic acid (10 mM), single H_2O_2/ascorbic acid system (the concentration of H_2O_2, 50 mM and the concentration of ascorbic acid, 10 mM). All the tests were performed at the temperature of 30 °C for 60 min.

2.4. Effect of reaction conditions on the molecular weights (Mw) of depolymerized product.

The effects of the following parameters were investigated: ultrasound intensity (3.8, 7.6, 11.4 and 15.2 W/mL), temperature (20, 30, 40 and 50 °C) and ascorbic acid concentration (1.0, 10, 50 and 100 mM). The general depolymerization conditions of all treatments were as follow: reaction time of 60 min, temperature at 30 °C, ascorbic acid concentration of 10 mM, hydrogen peroxide of 50 mM, the ultrasound intensity of 3.8 W/mL. The Mw of pectin samples were determined by gel permeation chromatography (GPC) according to our previously studies, with some modifications (Guo, et al., 2014). The average Mw determination was performed on a LC-20A HPLC system (Shimadzu, Kyoto, Japan) with an Ultrahydrogel 250 column (Waters, Milford, USA). Forty microliters of the sample solution were injected and eluted by 0.2 M NaCl at a flow rate of 0.5 mL/min. Standard dextrans (Sigma-Aldrich Chemical Co., St. Louis, MO, USA) having different molecular weights (from 0.5 to 670 kDa) were used to obtain calibration curves.

183 *2.5. Estimation of hydroxyl radicals.*

184 A method, based on the reaction of deoxyribose with HO• radicals (Verma et al.,
185 2003), was used for the study of the time course of production of HO• radicals by the
186 optimized ultrasound/H_2O_2/ascorbic acid system. Aliquots of the reaction mixture (450 µL)
187 were taken at different time intervals and supplemented with 50 µL deoxyribose (28 mM).
188 The reaction was stopped by the addition of 500 µL thiobarbituric acid (1% w/v in 50 mM
189 NaOH) and 500 µL of trichloroacetic acid (2.8% w/v) after 5 min of incubation. The
190 deoxyribose degradation product reacted with thiobarbituric acid during a subsequent 30
191 min incubation at 80 °C, with the resulting formation of a pink compound. The product of
192 the reaction was quantified by spectrophotometry (λ = 532 nm) after dilution with an equal
193 amount of water. The relative amount of HO• radicals detected was expressed in
194 absorbance units.

195

196 *2.6. Determination of hydroxyl radicals by ESR spin-trapping technique.*

197 ESR measurements were performed on an X-band ESR spectrometer (JES-FA-200;
198 JEOL, Tokyo, Japan) at room temperature. The measurement conditions were as follows:
199 field sweep, 317.7 to 327.7 mT; field modulation frequency, 100 kHz; field modulation
200 width, 0.1 mT; amplitude, 2; sweep time, 4 min; time constant, 0.03 s; microwave
201 frequency, 9.054 GHz; microwave power, 0.998 mW. All experiments were performed in
202 triplicate at room temperature.

2.7. Determination of monosaccharide composition.

Monosaccharide composition of oligosaccharide fragments was determined by the 1-phenyl-3-methyl-5-pyrazolone (PMP) high performance liquid chromatography (HPLC) method (Wu et al., 2013). Briefly, approximately 2 mg of pectin samples was hydrolyzed with 4 M trifluoroacetic acid (TFA) at 110 °C for 8 h. After cooling to room temperature, TFA was then removed and the reaction solution was adjusted to pH 7.0 with 2 M NaOH, and then with 0.3 M NaOH. The hydrolysate was derivatized with 50 μL of 0.3 M NaOH and 50 μL of 0.5 M PMP solution at 70 °C for 100 min. Chloroform was used to extract the hydrolysate and the hydrolysate was analyzed by a Waters 2695 HPLC system (Waters, USA) with an ZORBAX Eclipse XDB-C18 column (Agilent, 5 μm, 4.6 mm × 250 mm, Santa Clara, CA, USA). Mobile phase A was aqueous containing sodium phosphate buffer (0.05 M, pH 6.9) and acetonitrile (v/v; 85:15) and mobile phase B was aqueous containing sodium phosphate buffer (0.05 M, pH 6.9) and acetonitrile (v/v; 60:40). The time program of HPLC analysis was 0→10→30 min and the concentration program was 0→8%→20% of the mobile phase B at a flow rate of 1 mL/min and the samples were detected by UV detection at 250 nm, and the injection volume was 20 μL.

2.8. IR spectral analysis.

The FT-IR analysis was applied to obtain IR spectra of the pectin samples using a Nicolet Avatar 370 instrument. Samples (~1 mg) were ground together with 200 mg KBr,

223 pressed into pellets for IR scanning from 400 to 4000 cm^{-1} with 32 scans and a 4
224 cm^{-1} resolution. The degree of esterification and other functional groups were determined.
225
226 *2.9. NMR analysis of low-molecular-weight pectin.*
227 For NMR analysis, citrus pectin and LMP fractions (~5 mg) were evaporated with 550
228 μL of D_2O (99.96%) twice by vacuum freeze drying before final dissolution in 550 μL of
229 D_2O (99.96%). The samples were acquired in D_2O with chemical shifts expressed as δ
230 PPM, using the resonances of CH_3 groups of acetone (δ 30.2/2.22) as internal reference.
231 NMR spectra were collected by a 600 MHz NMR spectrometer (DD2-600; Agilent
232 Technologies Inc., CA, US) at 25 °C. The spectra were processed using the MestReNova
233 6.1.1 (MestreLab Research, Santiago de Compostela, Spain).
234
235 *2.10. Cell viability assay.*
236 The antitumor activity of PPs and LMWP on MCF-7 cells was evaluated using the
237 tetrazolium salt 3-(4,5-dimethylthiazol-2-yl)-2,5-diphenyltetrazolium bromide (MTT)
238 assay (Miao et al., 2013). The cells were incubated in Dulbecco's modified eagle medium
239 (DMEM) supplemented with 10% fatal bovine serun (FBS), 100 U/mL of penicillin and
240 100 g/mL of streptomycin at 37 °C in a humidified incubator at 5% CO_2. Briefly, 100 μL of
241 the cells were incubated in a 96-well plate at a concentration of 2×10^5 cells/mL. After 24 h
242 of cultivation, various concentrations of PPs and LMP (0, 10, 50, 100, 250 and 500 μg/mL)

were added slowly into the 96-well plate and cultured for 48 h. Fluorouracil (5-FU, 50 μg/mL) served as the positive control. At the end of each treatment, 20 μL of MTT (5 mg/mL) was added and the tumor cells were further incubated for 4 h for the formation of the formazan crystals. A volume of 100 μL DMSO was added to each well to dissolve the formazan crystals after the medium was removed. Subsequently, absorbance was measured at 570 nm with a microplate reader (Thermo multiscan Mk3, Thermo Fisher Scientific Inc., USA). The cell viability was expressed as

Cell viability (% control) = $[(A_s - A_b)/(A_c - A_b)] \times 100$

where A_c and A_b were the absorbance of the system without the addition of polysaccharides or 5-FU and cells, respectively, and As was the absorbance of the system only with polysaccharides or 5-FU.

2.11. Lactate Dehydrogenase (LDH) Assay

The cytotoxicity of the samples was assessed by measuring the release of lactate dehydrogenase (LDH) into the culture medium as an indicator of cell membrane injury 30 using a commercial LDH assay kit (Jiancheng BioEngineering, Nanjing, China) according to manufacturer's instructions. Briefly, at the end of the incubation period, 20 μL supernatant of the culture medium from different treatments was used to assess LDH leakage into the media. Subsequently, absorbance was measured at 440 nm with a

microplate reader (Thermo multiskan Mk3, Thermo Fisher Scientific Inc., USA). The LDH release ratio (% control) was expressed as;

LDH release ratio (% control) = $[(A_s-A_b)/(A_c-A_b)] \times 100$

where A_c and A_b were the absorbance of the system without the addition of polysaccharides or 5-FU and cells, respectively, and As was the absorbance of the system only with polysaccharides or 5-FU.

3. Results and discussion

3.1. The synergetic effects of sonolysis and H_2O_2/ascorbic acid system to depolymerize pectic polysaccharide.

We first examined whether H_2O_2/ascorbic acid each used on its own could depolymerize PPs. The results (**Figure 1a**) suggested H_2O_2/ascorbic acid could depolymerize PPs and reduce their average molecular weight from 791 kDa to 15.27 kDa in 60 min. In stark contrast, a 60 min treatment with ultrasound or H_2O_2 alone resulted in no apparent reduction of molecular weight. Interestingly, when H_2O_2 was combined with ultrasound the molecular weight of pectin polysaccharides could be reduced to below 20 kDa. These results suggest that while H_2O_2/ascorbic acid system is an efficient system to generate LMPs, ultrasound enhances the efficiency of free radical depolymerization.

Further studies on ultrasound enhanced H_2O_2/ascorbic acid depolymerize PPs showed that not only that the degradation process was accelerated but also the

282 degradation efficiency was greatly improved with the appearance of 14.26 kDa products
283 within 10 min.
284
285 *3.2. Effects of reaction parameters on pectic polysaccharide depolymerization.*
286 The effect of reaction temperature, ascorbic acid concentration, and ultrasonic
287 intensity during the depolymerization process on the degradation efficiency was
288 examined to optimize the depolymerization conditions. A neutral pH was applied in the
289 present study to prevent the acidic or basic hydrolysis of the polysaccharides, as the
290 branching chain may important for the activity of the PPs.
291 Increased temperatures result in higher average kinetic energy as a result of more
292 molecular collisions per unit time (Yue et al., 2008). Furthermore, cavitation bubbles
293 formed during the ultrasonic treatment can degrade organics (Golash & Gogate, 2012).
294 As a result, degradation efficiency increased markedly by elevating the reaction
295 temperature from 20 to 40 °C (**Figure 1b**). However, no obvious improvement in
296 degradation efficiency was observed when the temperature was increased to 50 °C. At
297 high temperatures, the concentrations of both H_2O_2 and ascorbic acid can be reduced due
298 to their self-decomposition, thus, decreasing degradation efficiency. Therefore, 40 °C was
299 selected as the optimal reaction temperature.
300 Reaction rates accelerate with the increasing concentrations of reactants. When the
301 concentration of H_2O_2 was 50 mM, increasing ascorbic acid concentration from 1 to 10

mM increased the degradation efficiency due to the increasing amount of HO•. Nevertheless, when the ratio of the concentration of H_2O_2 to the concentration of ascorbic acid was < 5, higher concentrations of ascorbic acid (>10 mM) were not effective for the depolymerization of PPs (**Figure 1c**). Under these reaction conditions, excess ascorbic acid (H_2A) is susceptible to autoxidation to generate dehydroascorbic acid anions (Eqs. (1) and (2)) that react with HO•, generated from H_2O_2/ascorbic acid redox system (Eq. (3)), (Bai & Wang, 1998) resulting in a decrease in depolymerization efficiency. Therefore, 10 mM ascorbic acid was considered as the appropriable concentration.

$$H_2A \rightarrow HA^- + H \quad (1)$$

$$HA^- + O_2 \rightarrow A^-\bullet + O_2^- + H^+ \quad (2)$$

$$HA^- + HO\bullet \rightarrow A^-\bullet + H_2O \quad (3)$$

Ultrasound intensity has been used as an important operational parameter in ultrasonic processes for controlling the formation of HO• radicals and cavitation bubbles (Joseph, Puma, Bono, & Krishnaiah, 2009). Degradation efficiency increases with increasing ultrasound intensities from 3.8 to 11.4 W/mL (**Figure 1d)**. Nevertheless, no further obvious improvement was detected when the ultrasound intensity was increased to 15.2 W/mL. In contrast to the ultrasound in the metal-catalyzed Fenton chemistry for pectin depolymerization, which mainly functions as a catalyst accelerating pectin depolymerization (Zhi, et al., 2017), the ultrasound (3.8-11.4 W/mL) in the H_2O_2/ascorbic acid system ultrasound reaction acts as both a catalyst, accelerating the generation of free

radicals, and also significantly changes the end point of the reaction. Ultrasound of 11.4 W/mL was selected as a suitable value to maximize conversion.

Based on results obtained, we set the optimal values of 40 °C, 10 mM, 11.4 W/mL as our reaction conditions. Ultrasound/H_2O_2/ascorbic acid was used to generate hydroxyl radicals in subsequent experiments. The involvement of hydroxyl radicals during PPs depolymerization is similar to the depolymerization of PPs by copper (II) and hydrogen peroxide. Hydroxyl radicals react with PPs by abstracting a hydrogen atom, leading to the sugar chain scission (Zhi et al., 2017).

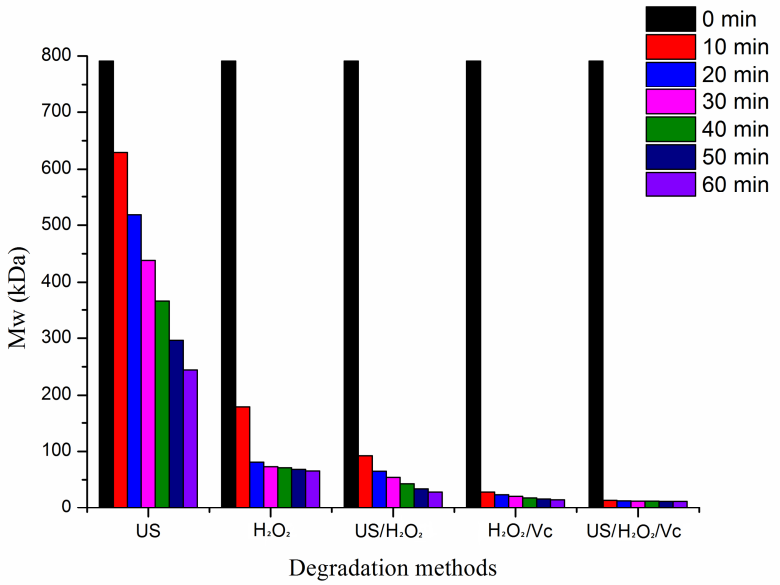

(a)

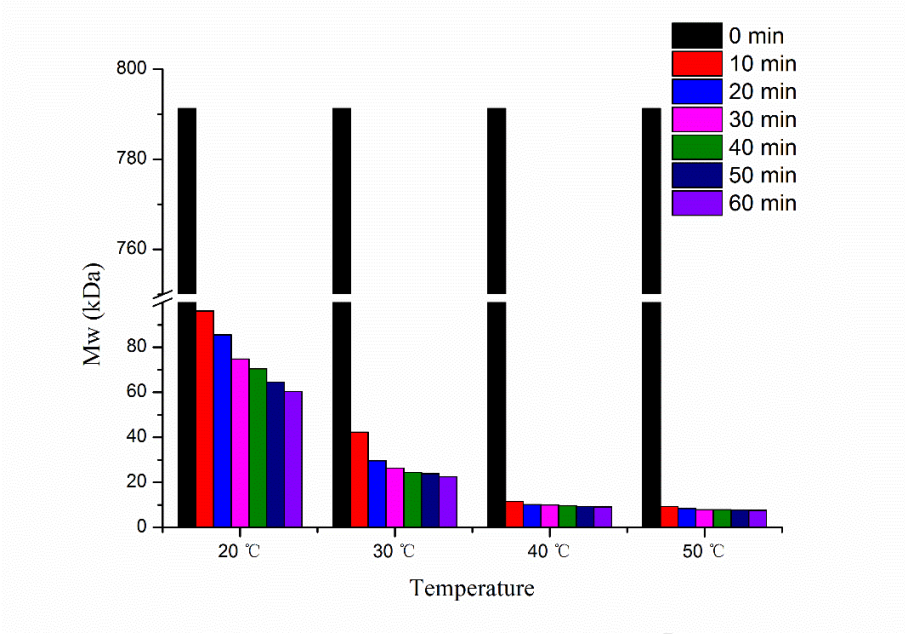

332

333 (b)

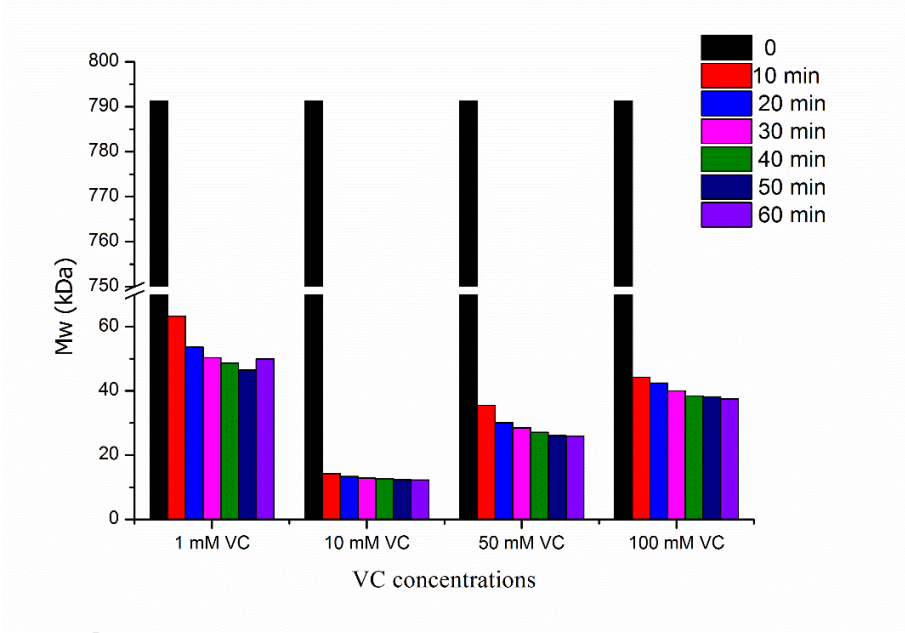

334

335 (c)

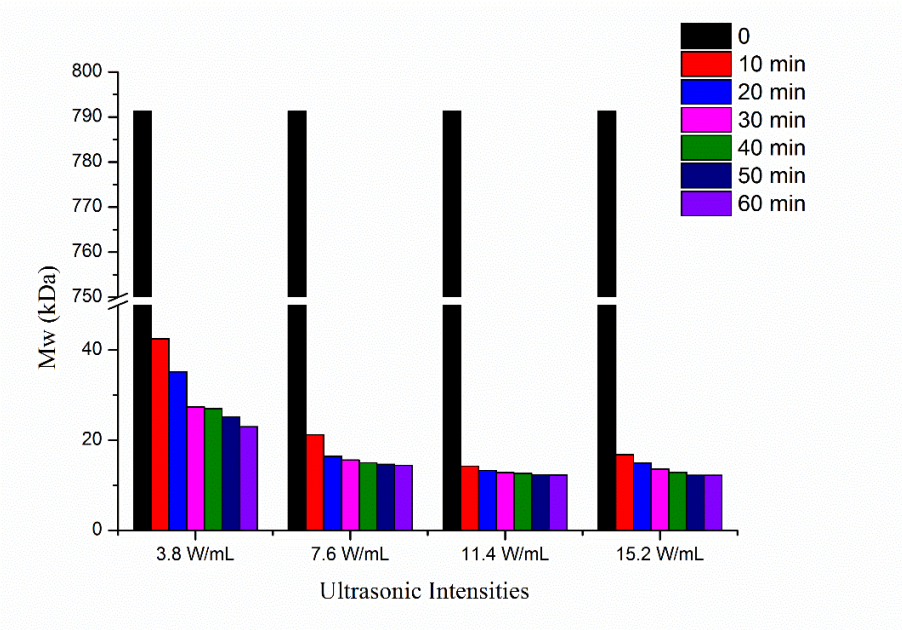

(d)

Figure 1. Effect of different reaction conditions on the molecular weights of depolymerized pectic polysaccharides: (a) different degradation systems (ultrasound alone; H_2O_2 alone; ultrasound in combination with H_2O_2; H_2O_2/ascorbic acid redox system; ultrasound in combination with H_2O_2/ascorbic acid system); (b) reaction temperature (temperature, 20 °C, 30 °C, 40 °C or 50 °C; H_2O_2 concentration, 50 mM; ascorbic acid concentration, 10 mM; ultrasound intensity, 3.8 W/mL); (c) ascorbic acid concentration (1 mM, 10 mM, 20 mM or 100 mM; H_2O_2 concentration, 50 mM; temperature, 30 °C; ultrasound intensity, 3.8 W/mL); (d) ultrasound intensity (intensity, 3.8 W/mL, 7.6 W/mL, 11.4 W/mL or 15.2 W/mL; H_2O_2 concentration, 50 mM; ascorbic acid concentration, 10 mM, temperature, 30 °C).

3.3. Estimation of hydroxyl radicals.

Ultrasound/H_2O_2/ascorbic acid is an effective and environmentally friendly method to depolymerize PPs. The system produces hydroxyl radicals during the reaction and the involvement of hydroxyl radicals during the depolymerization of PPs is similar to decolorization of dyes by ascorbic acid, copper (II) and hydrogen peroxide (Verma et al., 2003). HO• radicals have an unpaired electron making them strong oxidizing agents that react with polysaccharides causing their degradation. The concentration of HO• radicals in the ultrasound/H_2O_2/ascorbic acid system is the highest during the reaction, which explains the efficient degradation of PPs under these conditions **(Figure 2)**. The concentration of HO• radicals in the absence of ultrasound is obviously lower than that observed in the ultrasound/H_2O_2/ascorbic acid system. In the absence of ascorbic acid the amount of HO• radicals is considerably lower. It has been widely acknowledged that low frequency ultrasonic degradation of most water-soluble polymers in aqueous solutions is mainly attributed to the almost midpoint scission by mechanical effects induced by ultrasound (Koda, Taguchi, & Futamura, 2011). Our results indicate that low frequency ultrasound can also act as special catalyst to speed up and increase the total production of HO· radicals using non-metal Fenton chemistry, resulting in higher PPs depolymerization.

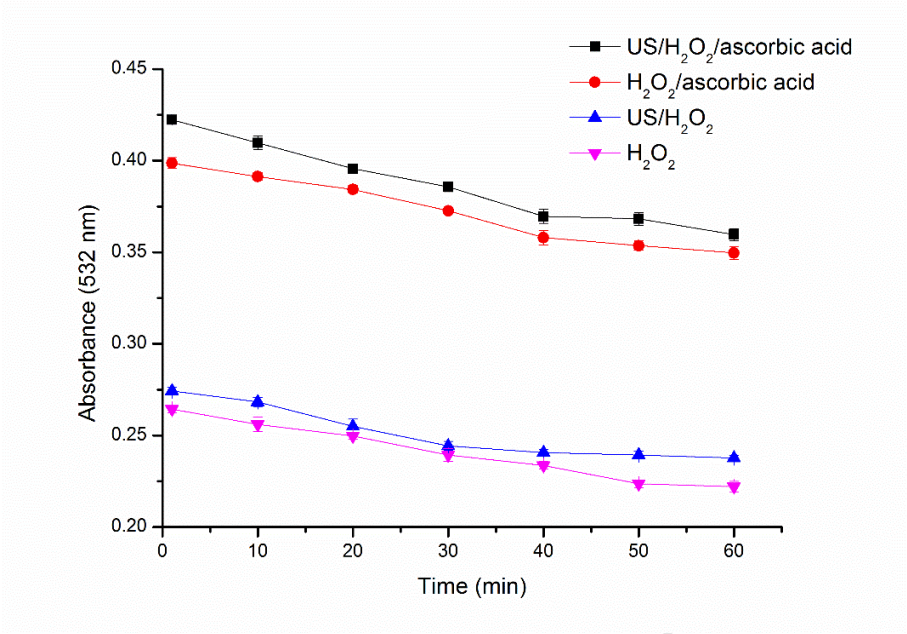

366

367 Figure 2. Concentrations of hydroxyl radicals during the incubation of H_2O_2 (50 mM) + ascorbic acid
368 (10 mM)/H_2O_2 (50 mM) in the presence and absence of ultrasound (11.4 W/mL). The concentration is
369 expressed as absorbance of the deoxyribose degradation product with thiobarbituric acid.

370 Electron spin resonance (ESR) technique was employed to detect HO• in the
371 different reaction systems. The spin adduct 5,5-dimethyl-1-pyrroline N-oxide
372 (DMPO)-OH, an adduct of DMPO and the hydroxyl radicals, was assigned based on
373 hyperfine coupling constants (hfcc). The hfcc are aH = aN = 1.49 mT, which is
374 consistent with those of previous reports (Mokudai, Nakamura, Kanno, & Niwano, 2012).
375 Relatively weak signals from DMPO-OH were detected in both H_2O_2 and
376 ultrasonic/H_2O_2 systems (**Figure 3**). The addition of ascorbic acid resulted in the
377 appearance of a strong signal from DMPO-OH and further increase of ultrasound energy
378 enhanced the signal from DMPO-OH. These ESR spectra suggest that the amount of

379 hydroxyl radical produced by the H_2O_2/ascorbic acid system was significantly higher
380 than that of H_2O_2 alone or ultrasound/H_2O_2 and that ultrasound could increase the
381 concentration of hydroxyl radicals in the H_2O_2/ascorbic acid system. These data are
382 consistent with the hydroxyl radical concentration estimated in the assay above.

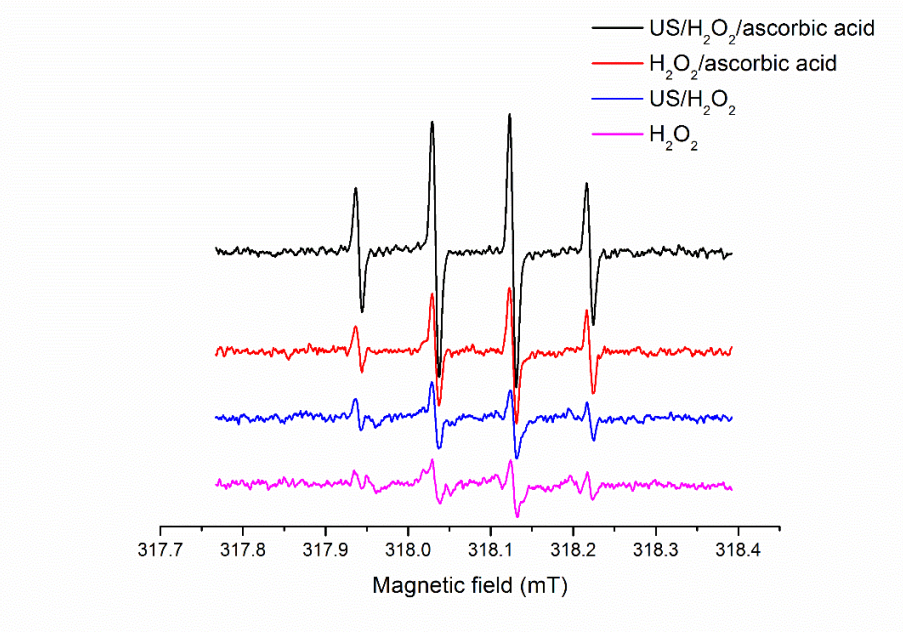

383

384 Figure 3. ESR spectra of reaction solution under different systems. H_2O_2 (50 mM); US (11.4
385 W/mL)/H_2O_2 (50 mM); H_2O_2 (50 mM)/ascorbic acid (10 mM); US (11.4 W/mL)/H_2O_2 (50
386 mM)/ascorbic acid (10 mM).

387

388 *3.4. Monosaccharide composition analysis.*

389 During the optimization process, three forms of degraded PPs with distinct
390 molecular weights were obtained. PPs were depolymerized under optimized conditions
391 from 791 kDa to 12.26 kDa (LMP2) within 60 min. Under milder (20 °C, 10 mM, 11.4

392 W/mL) and more severe (50 °C, 10 mM, 11.4 W/mL) conditions, relatively higher
393 molecular weight (60.33 kDa) (LMP1) and lower molecular weight (7.65 kDa) (LMP3)
394 products were obtained, respectively.

395 Chemical compositional analysis indicated that GalA (in mole%) was the principle
396 component of the four polysaccharides, while arabinose (Ara) and galactose (Gal) were
397 the major neutral saccharides. All chemical compositions, determined in the native PPs,
398 were also detected in each of the three depolymerized products, suggesting that
399 ultrasound/H_2O_2/ascorbic acid system did not alter the types of monosaccharides present.
400 With decreased molecular weights the total mole percentage of neutral monosaccharides
401 increased and the GalA content decreased (**Table 1)**, suggesting that chain breakage
402 might occur at GalA residues.

403 All four samples were relatively rich in homogalacturonans (HG) as opposed to
404 rhamnogalacturonans (RG), as deduced from the Rha/GalA ratio (Arnous & Meyer, 2009).
405 The low ratio of 0.51 determined for the native PPs indicates that both the
406 homogalacturonans and rhamnogalacturonans are predominate, whereas the increasing
407 ratio, close to 1, for three depolymerized products suggests that these contain a majority of
408 rhamnogalacturonan with a repeating unit of [→2)-α-L-Rha*p*-(1→4)-α-D-Gal*p*A-(1→]
409 (where *p* is pyranose). The ratio of (Ara + Gal) to Rha was calculated to estimate the
410 relative importance of the neutral side-chains to the rhamnogalacturonan backbone. These
411 ratios were at 5.48, 5.32, 5.04, 4.96 for PP, LMP1, LMP2 and LMP3, respectively. The

412 ratios Rha/GalA and (Ara + Gal)/Rha indicate that free radicals generated preferentially
413 attack GalA residues in the HG region of PPs, which was similar to the reported preference
414 for free radical depolymerization of pectin catalyzed by ultrasound-Fenton chemistry (Zhi
415 et al., 2017). Thus, this method might be applicable for the rapid preparation of RG-I
416 enriched LMPs.

417 Table 1. Monosaccharide composition of different pectin polysaccharides.

Monosaccharides (mol%)	PPs	LMP1	LMP2	LMP3
Ara	44.55±1.08	47.95±1.14	47.46±1.33	48.2±1.46
GalA	22.3±0.92	17.32±0.86	15.43±0.68	14.36±0.63
Gal	18.4±0.24	18.74±0.18	18.82±0.36	18.58±0.16
Rha	11.49±0.08	12.54±0.24	13.16±0.13	13.46±0.09
Fuc	2.3±0.16	2.34±0.08	3.91±0.28	4.22±0.11
Xyl	0.91±0.03	1.11±0.05	1.22±0.08	1.18±0.14
(Ara+Gal)/Rha	5.48	5.32	5.04	4.96
Rha/GalA	0.512	0.72	0.85	0.94

418

419 *3.5. Degradation products analysis by IR.*

420 The infrared spectra of the four samples are provided in **Figure 4**. Both native PPs and
421 its depolymerized products display similar spectral bands as IR is relatively insensitive to
422 minor structural changes in large polymer molecules. The major absorption at around
423 3405 cm^{-1} can be attributed to stretching of hydroxyl groups. The peak at around 3422 cm^{-1}
424 corresponds to C–H absorption, including CH, CH_2 and CH_3 stretching and bending
425 vibrations and an absorption at 2932 cm^{-1} is assigned to CH stretching of CH_2 groups. The
426 degree of methylation (DM) of pectin can be estimated by dividing the signal ascribed to

carboxylic ester by the sum of the signal ascribed to carboxylic ester and carboxylic acid groups (Fellah, 2009; Gnanasambandam, 2000). Signals at 1609 cm^{-1} can be attributed to the C=O stretching vibration of ionic carboxyl groups and no absorption corresponding to carboxylic ester could be found, indicating the absence of esterified pectins. The three absorption peaks between 1010 and 1150 cm^{-1} indicated the presence of pyranose (Zhang, 2013) and the pyranose configuration of the pectin did not change after ultrasound/H_2O_2/ascorbic acid treatment.

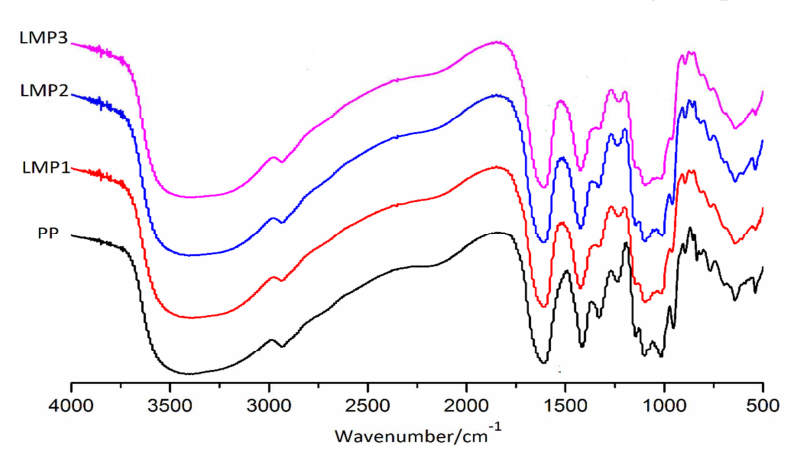

Figure 4. IR spectra (% transmittance as a function wavenumber) of native PPs and LMPs prepared by ultrasound/H_2O_2/ascorbic acid process. LMP1, LMP2 and LMP3 were prepared by US/H_2O_2/ascorbic acid system (ultrasound intensity, 11.4 W/mL; H_2O_2 concentration, 50 mM; ascorbic acid concentration, 10 mM) in 20 ℃, 30 ℃ and 50 ℃, respectively.

3.6. NMR spectra.

The ^{1}H NMR spectra of PP, LMP1, LMP2 and LMP3 were obtained to better understand the structural change of PPs during oxidation (**Figure 5**). In comparison, the depolymerized pectins exhibited similar spectra to the native polysaccharides, containing characteristic signals. Specifically, the signals at 1.31 ppm and 1.24 ppm were derived from methyl groups of L-rhamnose and were assigned to the *O*-2- and *O*-2,4-linked rhamnose, respectively (Zhi et al., 2017). In the anomeric region, the signals from 5.05-5.3 ppm correspond to the anomeric protons of Ara and signals at 5.29 ppm and 4.67 ppm were assigned to the H-1 of Rha and H-1 of Gal, respectively.

Some changes were observed following depolymerization. Signals at 4.01 ppm and 4.46 ppm, assigned to the H-3 and H-4 of GalA, respectively, showed a substantial decrease in intensity under more stringent reaction conditions, suggesting the selective cleavage of GalA. These results are in agreement with those from the monosaccharide compositional assay (Section 3.4). Thus, based on the ^{1}H NMR data, it can be reasonably inferred that the reaction temperature is the most important factor in the system and HO • generated by ultrasound/H_2O_2/ascorbic acid process selectively attacks the glycosidic bond without damaging the RG-I region of PPs, similar to metal-catalyzed Fenton chemistry (Bokare & Choi, 2014).

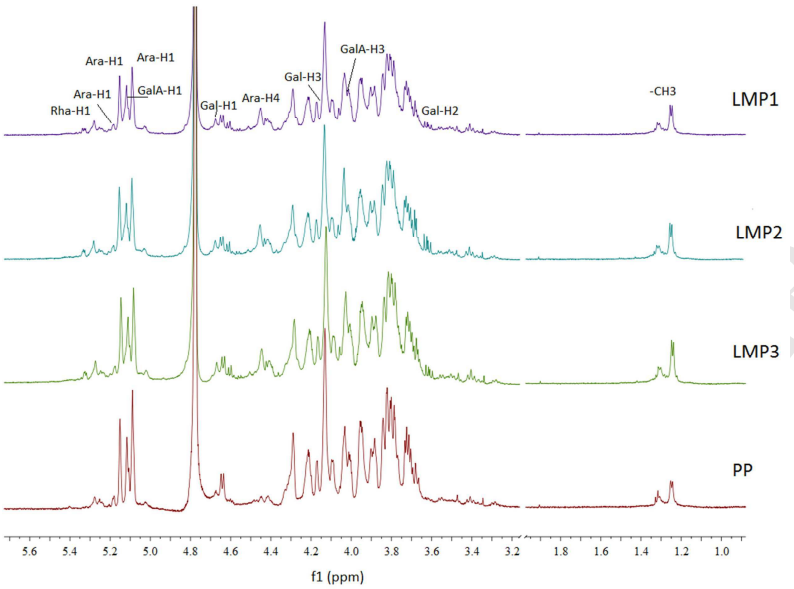

458

459 Figure 5. ^{1}H NMR spectra (intensity and a function of chemical shift in ppm) of PPs and LMPs.
460 LMP1, LMP2 and LMP3 were prepared by US/H_2O_2/ascorbic acid system (ultrasound intensity, 11.4
461 W/mL; H_2O_2 concentration, 50 mM; ascorbic acid concentration, 10 mM) in 20 °C, 30 °C and 50 °C,
462 respectively.

463 Due to the limited resolution of the ^{1}H NMR spectra of the polysaccharide mixtures,
464 2D NMR was employed to further determine the structure of LMP3 as a representative
465 product. The assignments of ^{1}H and ^{13}C chemical shifts (**Table 2**) were made from total
466 correlation spectroscopy (TOCSY) **(Figure 6a),** heteronuclear single quantum coherence
467 (HSQC) spectra (**Figure 6b**) and nuclear Overhauser effect spectroscopy (NOESY)
468 (**Figure 6c**). The analysis of the COSY and TOCSY revealed the residues with α- and
469 β-galactopyranosidic, α-rhamnopyranosidic and α-arabinofuranosidic configuration. The
470 HSQC spectrum showed that the residue with α-galacto-configuration corresponded to

471 the α-galactopyranosyl uronic acid residues substituted at position 4 (Bushneva, Ovodova,
472 Shashkov, & Ovodov, 2002) and α-arabinofuranosidic residues were both non-substituted
473 C5 (64.81 ppm) and 5-subsituted (C5 72.5 ppm). The correlation peak of H1/H4
474 (5.12/4.46) of the GalA residues in the NOESY spectrum further confirmed the presence
475 of α-1,4-linked galactopyranosyl uronic acid residues. The correlation peaks of
476 H1(Gal*p*A)/H2(Rha*p*) at 5.12/4.32ppm, H1(Ara*f*)/H4(Rha*p*) (where *f* is furanose) at
477 5.14/4.45 ppm and H1(Gal*p*)/H4(Rha*p*) at 4.67/4.45 ppm in NOESY spectra indicated
478 that some GalA residues are linked to the 2-position of Rha residues and some Ara*f* and
479 Gal*p* residues are linked to the 4-position of Rha residues. In addition, the correlation
480 peak of H1(Rha*p*)/H4(Gal*p*A) at 5.29/4.46 ppm confirmed that the residues of
481 rhamnopyranose are linked to the 4-position of α-GalA residues. Observation of
482 correlation signals B1/B5 at 5.11/3.93 in the NOESY spectrum suggested the presence of
483 a fragment. . .→5)-Ara*f*-(1→5)-Ara*f*-(1→. . .. Correlation signal at D1/C3 (5.27/4.15 ppm)
484 led to an unambiguous identification of substitution of residue (C) by terminal *α*-Ara*f* at
485 C3.

486 Because LMP3 is a LMP mixture it is not possible to assign all of the signals in
487 NMR spectra. Based on the data obtained, we suggested that the core of the pectic
488 polysaccharide is composed of residues of α-1,4-galactopyranosyl uronic acid and
489 α-1,2-rhamnopyranose. The side chain of hair regions was represent different blocks
490 composed of residues of α-1,5- linked arabinofuranose and as well as β-1,4- linked

galactopyranose, consistent with previous reports that neutral fragments of arabinan and galactan are the most likely the side chain of pectic polysaccharides attached to the backbone of rhamnogalacturonan (Bushneva et al., 2002). Arabinogalactans (AG I, AG II) and possibly galactoarabinans are also typical neutral sugar side chains of branched RG I polysaccharides. The presence of β-1,3-linked-Gal*p* units also suggests the presence of arabinogalactans in LMP3 (Carlotto et al., 2016).

Table 2. 1H/13C NMR chemical shifts assignments of LMP3

Residue		Chemical shift (ppm)					
		H1 (C1)	H2 (C2)	H3 (C3)	H4 (C4)	H5 (C5)	H6 (C6)
→3)-α-Ara-(1→	A	5.17 (111.18)	4.47 (81.39)	4.11 (80.15)	4.15 (84.69)	3.77/3.83 (64.81)	-
→5)-α-Ara-(1→	B	5.11 (111.20)	4.31 (85.32)	4.13 (84.69)	4.19 (81.29)	3.83/3.93 (72.50)	-
→3,5)-α-Ara-(1→	C	5.14 (110.97)	4.41 (80.55)	4.15 (85.99)	4.45 (81.74)	3.83/3.95 (72.66)	-
α-Ara-(1→3	D	5.27 (113.67)	4.35 (81.74)	4.12 (86.36)	4.25 (85.99)	3.77/3.83 (68.37)	
→4)-α-GalA-(1→	E	5.12 (102.67)	3.95 (69.92)	4.01 (72.39)	4.46 (81.39)	4.69 (73.40)	-
→3)-β-Gal-(1→	F	4.65 (107.98)	3.69 (76.02)	4.18 (85.05)	4.29 (74.05)	3.72 (78.22)	3.75 (64.73)
→4)-β-Gal-(1→	F’	4.67 (107.98)	3.59 (77.06)	3.77 (72.05)	4.43 (80.96)	3.72 (78.22)	3.75 (64.73)
→2)→α-Rha-(1→	G	5.29 (102.27)	4.32 (80.39)	4.03 (72.62)	3.95 (73.03)	3.92 (72.62)	-
→2,4)-α-Rhap-(1→	G’	5.30 (102.27)	4.51 (81.74)	4.03 (72.62)	4.45 (82.52)	4.14 (73.98)	-

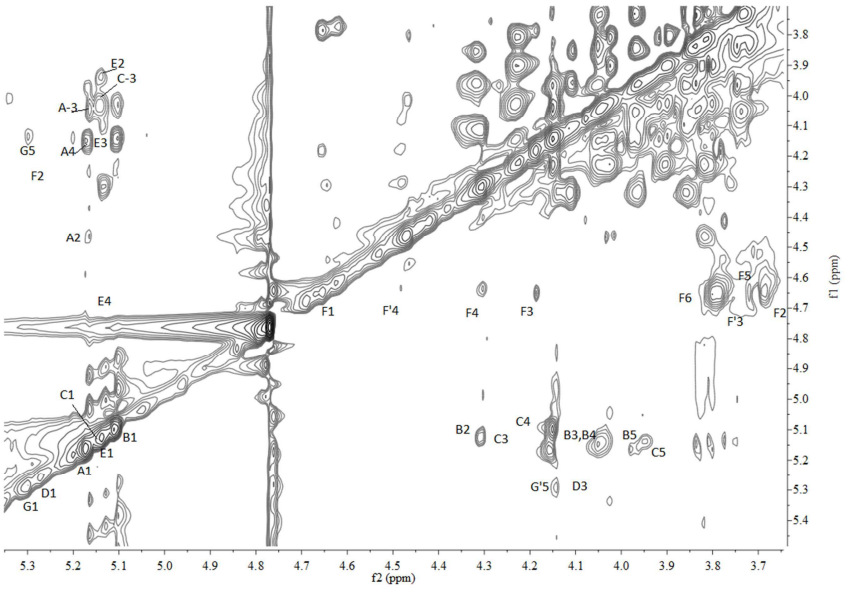

499

500 (a)

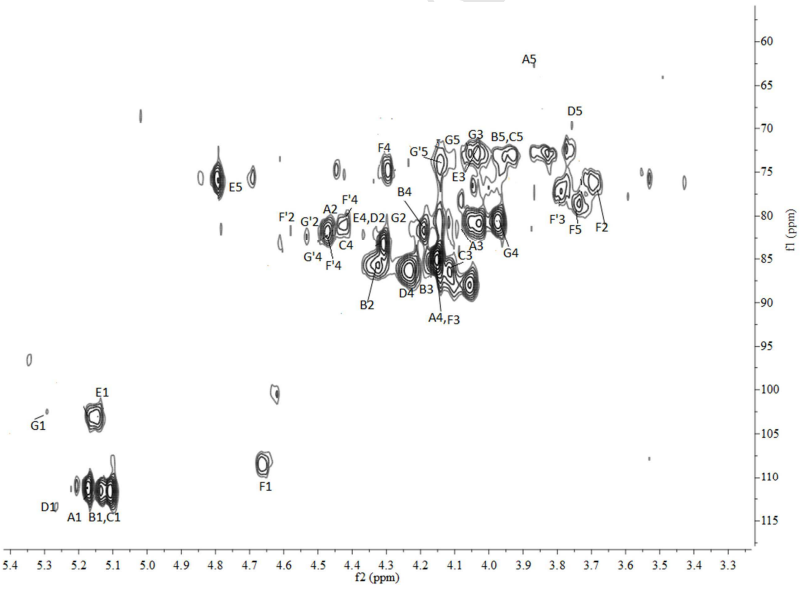

501

502 (b)

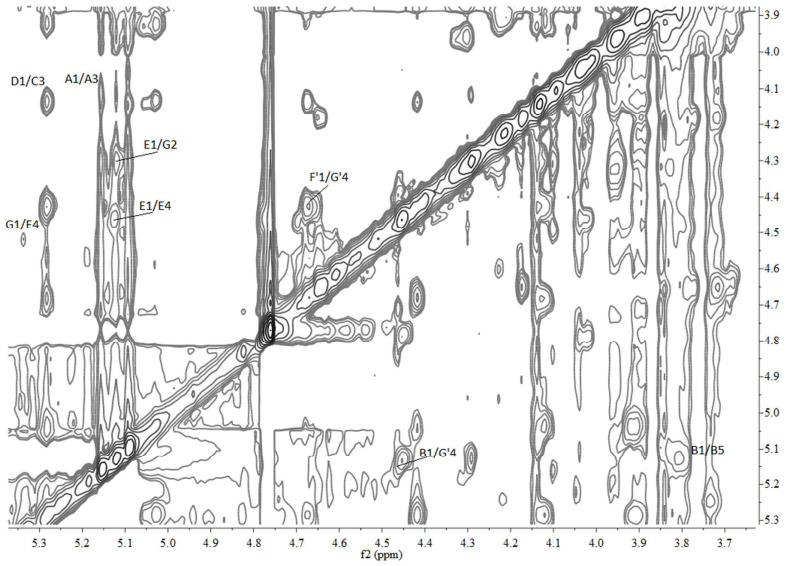

(c)

Figure 6. NMR spectra of LMP3 (a) TOCSY of LMP3; (b) HSQC of LMP3; (c) NOESY of LMP3. LMP3 were prepared by ultrasonic/H_2O_2/ascorbic acid system (ultrasound intensity, 11.4 W/mL; H_2O_2 concentration, 50 mM; ascorbic acid concentration, 10 mM; reaction temperature: 50 °C)

3.7. The proposed mechanism of pectic polysaccharide depolymerization by ultrasound/H_2O_2/ascorbic acid system.

Based on the detailed analysis of chemical composition, IR and NMR, the mechanism of ultrasound/H_2O_2/ascorbic acid process to generate RG-I enriched fragments can be proposed **(Figure 7**). The radical degradation process occurs through generation of free hydroxyl radical OH • by ultrasound/H_2O_2/ascorbic acid system. Ultrasound induces acoustic cavitation and the subsequent violent collapse of cavitation at multiple locations in the system can increase the temperature (about 5000 K) and

517 pressures (2000 atm) significantly in the collapsing bubble and close vicinity of the
518 bubble, which gives rise to generation of OH • and H • radicals, which can subsequently
519 form hydrogen peroxide (H_2O_2) (Eqs.(4)-(8)) (Czechowska-Biskup, Rokita, Lotfy,
520 Ulanski, & Rosiak, 2005; Gogate & Prajapat, 2015; Leonelli & Mason, 2010), resulting
521 in an additive effect of ultrasonic treatment and H_2O_2/ascorbic acid redox system,
522 generating more HO• radicals. In addition, the ultrasound can also lower activation
523 energy for H_2O_2 decomposition. The high temperature and pressures due to the
524 significant release of accumulated energy and hot spots when the bubble collapse can
525 significantly contribute to water ionization, leading to higher concentration of H^+ in the
526 system (Eq. (9)) (Marshall & Franck, 1981). The H^+ can interact with carbonyl group
527 (C=O) in the ascorbic acid and C1 becomes a positive carbon ion following the electron
528 redistribution. Electronic cloud density distribution of C3 decreases the generation of
529 extended pi bond with C1, thus, contributing to the complexation between C3 and
530 hydroxyl groups of H_2O_2 and redox reactions (Eq. (10)). It also has been reported that
531 ultrasound can depolymerize polysaccharide due to the physical effects (Zhang et al.,
532 2013). During the ultrasound treatment, the shear force can lead to the disaggregation of
533 polysaccharide clusters, especially in the early stage by breaking up the non-covalent
534 intra and inter-molecular bonds (Yan, Pei, Ma, & Wang, 2015) and the resulting flexible
535 structure makes the PPs more vulnerable to free radical attack. The reactive species
536 primarily attacks at the glycosidic bond and the GalA residues on the HG domain are

537 more reactive with hydroxyl radicals, resulting in chain scission and RG-I enriched
538 fragments, which is consistent with previous reports that alduronic acid (GalA and GlcA,
539 etc.) residues of polysaccharides are very susceptible to free radical degradation (Li et al.,
540 2016; Uchiyama, Dobashi, Ohkouchi, & Nagasawa, 1990; Zhang et al., 2013; Zhi et al.,
541 2017).

542 $H_2O \rightleftarrows H\bullet + HO\bullet$ (4)

543 $H\bullet + O_2 \rightleftarrows HO_2\bullet$ (5)

544 $H\bullet + HO_2\bullet \rightleftarrows H_2O_2$ (6)

545 $HO\bullet + HO\bullet \rightleftarrows H_2O_2$ (7)

546 $HO_2\bullet + HO_2\bullet \rightleftarrows H_2O_2 + O_2$ (8)

547 $H_2O \rightleftarrows H^+ + OH^-$ (9)

548 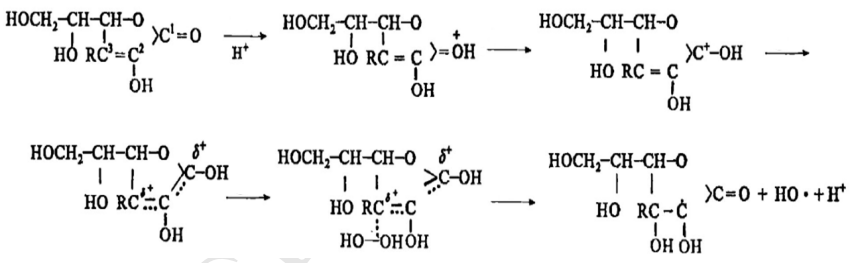 (10)

549 Free radical generation by ultrasound/H_2O_2/ascorbic acid system is also suitable for
550 ultrafast preparation of other low molecular weight polymers and has been helpful in
551 unraveling the structure of unknown polysaccharides.

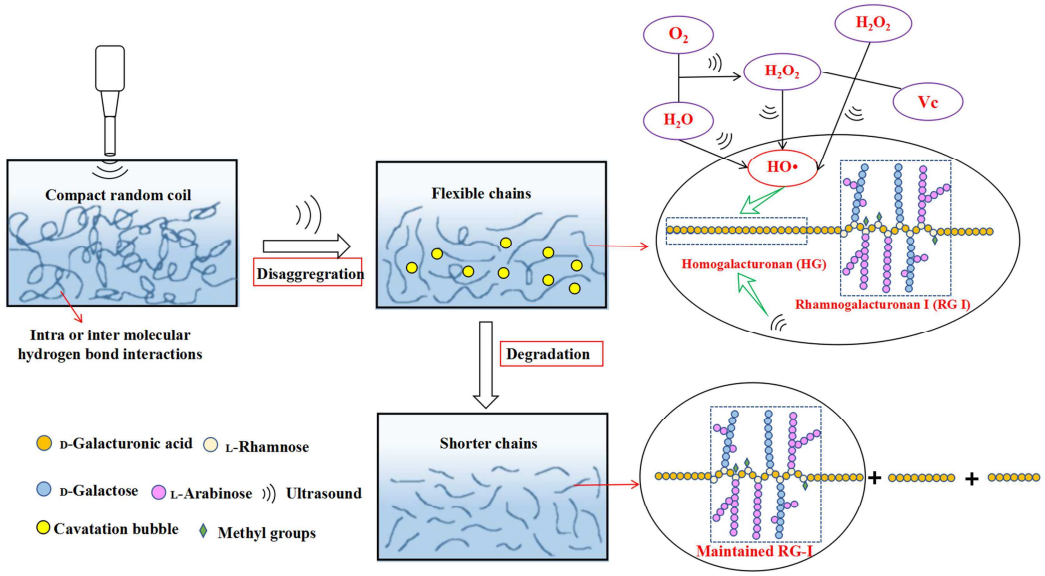

552

553 Figure 7. The schematic diagram of PPs degradation path by ultrasound/H_2O_2/ascorbic acid system.
554 The ultrasound enhances the efficiency of H_2O_2/ascorbic acid system to degrade PPs through both
555 chemical effects (increasing the amount of hydroxyl radicals and lowering activation energy of H_2O_2
556 decomposition) and mechanical effects (disaggregating polysaccharide clusters).

557

558 *3.8. Cell viability assay and cytotoxicity assay.*

559 The *in vitro* antitumor activity of both native PPs and LMP3 were determined at
560 different concentration (0, 10, 50 100, 250, 500 μg/mL) by examining the proliferation of
561 MCF-7 cells. LMP3 significantly inhibited the proliferation of MCF-7 cells and the
562 inhibitory effect increased in a concentration-dependent manner (**Figure 8a**). Intact PPs
563 exhibited a much lower inhibitory effect on MCF-7 cells proliferation. LMP3 showed the
564 highest proliferation-inhibitory effect against MCF-7 cells with a cell viability of 56.39 ±

565 2.47% at the concentration of 500 μg/mL. While native PPs exhibited moderate
566 anti-proliferation effect against MCF-7 cells at 500 μg/mL (34.71 ± 3.24%). Neither PPs
567 nor LMP3 were comparable to the positive control relying on 5-FU. Galactoside
568 containing molecules derived from pectin have been demonstrated to interact with a
569 galectin 3-type lectin at the surface of proliferating mammalian cancer cells (Bushneva et
570 al., 2002; Nangia-Makker et al., 2002), thus preventing tumor growth. Despite the similar
571 structures and compositions between the native PPs and LMP3, their antitumor activity
572 was distinct, suggesting the significance of molecular size in polysaccharide binding to
573 galectin-3 of cancer cells (Sathisha, Jayaram, Nayaka, & Dharmesh, 2007). Moreover, the
574 uptake of oligosaccharides by cancer cells was in a much better rate than that of intact
575 PPs from the same sources, thus affecting the antitumor activity (Kapoor et al., 2017).

576 LDH content is an indicator of loss in cell membrane integrity (G. X. Ma, et al.,
577 2014) and loss in membrane integrity occurs due to both necrosis and apoptosis death
578 events (Murthy, Jayaprakasha, Kumar, Rathore, & Patil, 2011). The cytotoxicity of the
579 two polysaccharides was evaluated to further confirm the proliferation inhibitory effect of
580 native PPs and LMP3 on MCF-7 cells. LDH release of MCF-7 cells into the medium was
581 significantly increased in a dose-dependent manner in the presence of the two
582 polysaccharides ($P<0.05$) (**Figure 8b**). The content of LDH release triggered by LMP3
583 treatment at 500 μg/mL for 48 h was 162.8 ± 5.12 % compared to the untreated cells,
584 much higher than that of PPs (138.3 ± 2.5%). The results above indicated that LMP3 was

585 endowed with higher cytotoxic effects against MCF-7 cells, which was consistent with

586 cell viability assay.

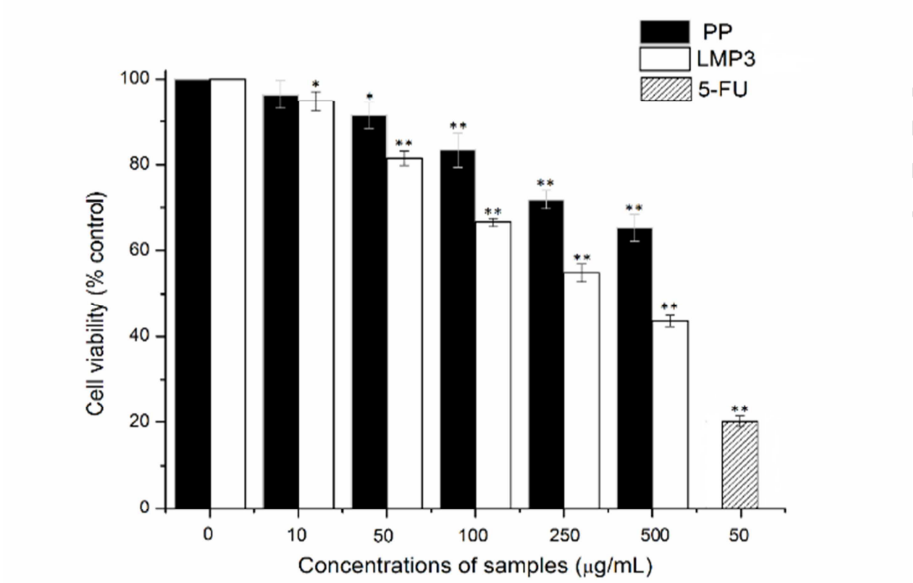

587

588 (a)

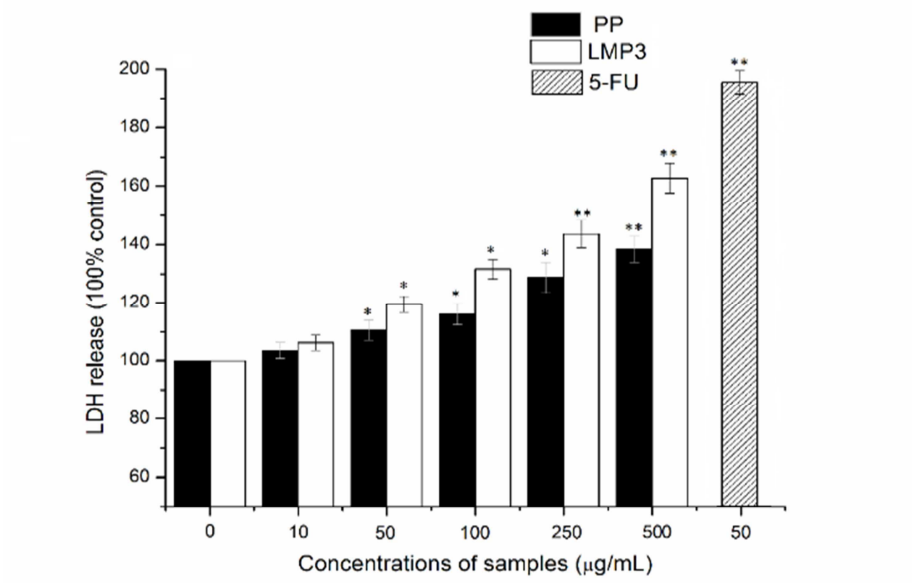

589

590 (b)

Figure 8. (a) Effects of native PPs and LMP3 on the proliferation of MCF-7 cells. Cells were cultured in the presence of PPs and LMP3 (10-500 μg/mL) for 48 h and the cell growth was determined by the MTT assay. (b) Cytotoxic effects of native PPs and LMP3 on MCF-7 cells. Cells were cultured in the presence of PPs and LMP3 (10-500 μg/mL) for 48 h and 20 μL supernatant of the culture medium was used to assess LDH leakage into the media. Data are presented as mean ± S.D. (*) $P < 0.05$ and (**) $P < 0.01$ indicate statistically significant differences versus blank control groups.

4. Conclusion

In the present study, an effective ultrasound accelerated non-metal Fenton redox system relying on H_2O_2/ascorbic acid was established for the controlled depolymerization of PPs recycled from citrus canning processing water and the antitumor activity of resulting fragment was determined. Ultrasound can disaggregate PP clusters by mechanical effects and ultrasound/H_2O_2/ascorbic acid system generates a greater concentration of hydroxyl radical, depolymerizing PPs within minutes with these free radicals preferentially cleaving the GalA in the HG region. Thus, the HG region of PPs decreases throughout the depolymerization. Structural analysis demonstrates that ultrasound/H_2O_2/ascorbic acid depolymerization of PPs affords RG-I enriched LMPs with a highly branched structure of arabinan. The *in vitro* antitumor activities of native PPs and LMP3 were examined using MTT and LDH assay. The results suggest that LMP3 exhibited significantly higher antitumor activity against MCF-7 human breast cells

611 compared to native PPs and that activity might be associated with their molecular size.
612 These results suggest that the LMPs obtained from citrus canning processing water might
613 be suitable for use in functional foods and potential therapeutic agents for human cancer.
614 Thus, the free radical depolymerization of PPs may provide effective streams for either
615 biological or industrial upgrading strategies aimed toward wastewater valorization.
616

617 **Acknowledgements**

618 This work was financially supported by the Key Research and Development Project
619 of Zhejiang Province, China (2015C02036) and Public Welfare Project of Zhejiang
620 Province, China (2015C32088).

621
622
623
624
625
626
627
628
629
630

631 **References**

632 Arnous, A., & Meyer, A. S. (2009). Quantitative prediction of cell wall polysaccharide
633 composition in grape (Vitis vinifera L.) and apple (Malus domestica) skins from
634 acid hydrolysis monosaccharide profiles. *Journal of Agricultural and Food*
635 *Chemistry, 57*(9), 3611-3619.
636 Bai, L., & Wang, J. (1998). Spin trapping - ESR study on the reaction of ascorbic acid with
637 hydrogen peroxide. *Chemical Journal of Chinese Universities, 19*, 890-894.
638 Belén Gómez, B. G., Remedios Yáñez, Henk Schols, & José L. Alonso (2016). Prebiotic
639 potential of pectins and pectic oligosaccharides derived from lemon peel wastes
640 and sugar beet pulp: A comparative evaluation. *Journal of Functional Foods, 20*,
641 108-121.
642 Bokare, A. D., & Choi, W. (2014). Review of iron-free Fenton-like systems for activating
643 H_2O_2 in advanced oxidation processes. *Journal of Hazardous Materials, 275*,
644 121-135.
645 Bushneva, O. A., Ovodova, R. G., Shashkov, A. S., & Ovodov, Y. S. (2002). Structural
646 studies on hairy region of pectic polysaccharide from campion Silene vulgaris
647 (Oberna behen). *Carbohydrate Polymers, 49*(4), 471-478.
648 Carlotto, J., Souza, L. M., Baggio, C. H., Werner, M. F. D., Maria-Ferreira, D., Sassaki, G.
649 L., Iacomini, M., & Cipriani, T. R. (2016). Polysaccharides from *Arctium lappa L.*:
650 chemical structure and biological activity. *International Journal of Biological*
651 *Macromolecules, 91*, 954-960.
652 Chen, J., Liang, R. H., Liu, W., Li, T., Liu, C. M., Wu, S. S., & Wang, Z. J. (2013).
653 Pectic-oligosaccharides prepared by dynamic high-pressure nnicrofluidization and
654 their in vitro fermentation properties. *Carbohydrate Polymers, 91*(1), 175-182.
655 Chen, J. L., Cheng, H., Wu, D., Linhardt, R. J., Zhi, Z. J., Yan, L. F., Chen, S. G., & Ye, X.
656 Q. (2017). Green recovery of pectic polysaccharides from citrus canning
657 processing water. *Journal of Cleaner Production, 144*, 459-469.
658 Dikeman, C. L., Fahey, G. C. (2006). Viscosity as related to dietary fiber: A review.
659 *Critical Reviews in Food Science and Nutrition, 46*, 649-663.
660 Czechowska-Biskup, R., Rokita, B., Lotfy, S., Ulanski, P., & Rosiak, J. M. (2005).
661 Degradation of chitosan and starch by 360-kHz ultrasound. *Carbohydrate*
662 *Polymers, 60*(2), 175-184.
663 Dogan, M., Kayacier, A., & Ic, E. (2007). Rheological characteristics of some food
664 hydrocolloids processed with gamma irradiation. *Food Hydrocolloids, 21*(3),
665 392-396.
666 Fellah, A., Anjukandi, P., Waterland, M.R., & Williams, M.A.K. (2009). Determining the
667 degree of methylesterification of pectin by ATR/FT-IR: methodology optimisation

668 and comparison with theoretical calculations. *Carbohydrate Polymers, 78*,
669 847-853.
670 Garna, H., Mabon, N., Wathelet, B., & Paquot, M. (2004). New method for a two-step
671 hydrolysis and chromatographic analysis of pectin neutral sugar chains. *Journal of*
672 *Agricultural and Food Chemistry, 52*(15), 4652-4659.
673 Garrido-Ramirez, E. G., Theng, B. K. G., & Mora, M. L. (2010). Clays and oxide minerals
674 as catalysts and nanocatalysts in Fenton-like reactions - A review. *Applied Clay*
675 *Science, 47*(3-4), 182-192.
676 Gnanasambandam, R., & Proctor, A. (2000). Determination of pectin degree of
677 esterification by diffuse reflectance Fourier transform infrared spectroscopy. *Food*
678 *Chemistry, 68*, 327-332.
679 Gogate, P. R., & Prajapat, A. L. (2015). Depolymerization using sonochemical reactors: A
680 critical review. *Ultrasonics Sonochemistry, 27*, 480-494.
681 Golash, N., & Gogate, P. R. (2012). Degradation of dichlorvos containing wastewaters
682 using sonochemical reactors. *Ultrasonics Sonochemistry, 19*(5), 1051-1060.
683 Grohmann, K., Cameron, R. G., & Buslig, B. S. (1995). Fractionation and pretreatment of
684 orange peel by dilute acid hydrolysis. *Bioresource Technology, 54*(2), 129-141.
685 Guo, X., Ye, X. Q., Sun, Y. J., Wu, D., Wu, N. A., Hu, Y. Q., & Chen, S. G. (2014).
686 Ultrasound effects on the degradation kinetics, structure, and antioxidant activity of
687 sea cucumber fucoidan. *Journal of Agricultural and Food Chemistry, 62*(5),
688 1088-1095.
689 Joseph, C. G., Puma, G. L., Bono, A., & Krishnaiah, D. (2009). Sonophotocatalysis in
690 advanced oxidation process: A short review. *Ultrasonics Sonochemistry, 16*(5),
691 583-589.
692 Kapoor, S., & Dharmesh, S. M. (2017). Pectic oligosaccharide from tomato exhibiting
693 anticancer potential on a gastric cancer cell line: Structure-function relationship.
694 *Carbohydrate Polymers, 160*, 52-61.
695 Karboune, S., & Khodaei, N. (2016). Structures, isolation and health-promoting properties
696 of pectic polysaccharides from cell wall-rich food by-products: a source of
697 functional ingredients. *Current Opinion in Food Science, 8*, 50-55.
698 Khalikov, D. K., & Mukhiddinov, Z. K. (2004). Physicochemical principles of plant-cell
699 protopectin decomposition by aced catalysts. *Chemistry of Natural Compounds,*
700 *40*(2), 101-114.
701 Khodaei, N., & Karboune, S. (2016). Enzymatic generation of galactose-rich
702 oligosaccharides/oligomers from potato rhamnogalacturonan I pectic
703 polysaccharides. *Food Chemistry, 197*, 406-414.
704 Khotimchenko, M., Kovalev, V., Kolenchenko, E., & Khotimchenko, Y. (2012). Acidic
705 method for the low molecular pectin preparation. *International Journal of*
706 *Pharmacy and Pharmaceutical Sciences, 4*, 279-28 3.

Koda, S., Taguchi, K., & Futamura, K. (2011). Effects of frequency and a radical scavenger on ultrasonic degradation of water-soluble polymers. *Ultrasonics Sonochemistry, 18*(1), 276-281.

Shin, K. S., Kiyohara, H., Matsumoto, T., & Yamada, H. (1997). Rhamnogalacturonan II from the leaves of Panax ginseng C.A. Meyer as a macrophage Fc receptor expression-enhancing polysaccharide. *Carbohydrate Research, 300*, 239-249.

Leclere, L., Cutsem, P. V., & Michiels, C. (2013). Anti-cancer activities of pH- or heat-modifed pectin. *Frontiers in Pharmacology, 4*, 1-8.

Leonelli, C., & Mason, T. J. (2010). Microwave and ultrasonic processing: Now a realistic option for industry. *Chemical Engineering and Processing, 49*(9), 885-900.

Levigne, S., Ralet, M. C., & Thibault, J. F. (2002). Characterisation of pectins extracted from fresh sugar beet under different conditions using an experimental design. *Carbohydrate Polymers, 49*(2), 145-153.

Li, J. H., Li, S., Zhi, Z. J., Yan, L. F., Ye, X. Q., Ding, T., Yan, L., Linhardt, R. J., & Chen, S. G. (2016). Depolymerization of fucosylated chondroitin sulfate with a modified Fenton-system and anticoagulant activity of the resulting fragments. *Marine Drugs, 14*(9), 1-13.

Li, L. C., Li, J., & Gao, J. (2014). Functions of galectin-3 and its role in fibrotic diseases. *Journal of Pharmacology and Experimental Therapeutics, 351*(2), 336-343.

Zhang, L. F., Ye, X. Q., Ding, T., Sun, X. Y., Xu, Y. T., Liu, & D. H. (2013). Ultrasound effects on the degradation kinetics, structure and rheological properties of apple pectin. *Ultrasonics Sonochemistry, 20*, 222-231.

Ma, G. X., Yang, W. J., Mariga, A. M., Fang, Y., Ma, N., Pei, F., & Hu, Q. H. (2014). Purification, characterization and antitumor activity of polysaccharides from Pleurotus eryngii residue. *Carbohydrate Polymers, 114*, 297-305.

Ma, X. B., Zhang, L. F., Wang, W. J., Zou, M. M., Ding, T., Ye, X. Q., & Liu, D. H. (2016). Synergistic Effect and mechanisms of combining ultrasound and pectinase on pectin hydrolysis. *Food and Bioprocess Technology, 9*(7), 1249-1257.

Marshall, W. L., & Franck, E. U. (1981). Ion product of water substance, O-degrees-C-1000-degrees-C, 1-10,000 bars - new international formulation and its background. *Journal of Physical and Chemical Reference Data, 10*(2), 295-304.

Hao, M., Cheng, H. R., Xue, H. T., Zhang, T., Zhou, Y. F., & Tai, G. H. (2013). Comparative studies on the anti-tumor activities of high temperature- and pH-modifed citrus pectin. *Food Function, 4*, 960-971.

Miao, S. S., Mao, X. H., Pei, R., Miao, S. P., Xiang, C., Lv, Y. J., Yang, X. G., Sun, J., Jia, S. S., & Liu, Y. P. (2013). Antitumor activity of polysaccharides from Lepista sordida against laryngocarcinoma in vitro and in vivo. *International Journal of Biological Macromolecules, 60*, 235-240.

745 Mokudai, T., Nakamura, K., Kanno, T., & Niwano, Y. (2012). Presence of hydrogen
746 peroxide, a source of hydroxyl radicals, in acid electrolyzed water. *PLoS One, 7*(9),
747 e46392.
748 Moreno, F. J., & Sanz, M. L. (2014). *Food oligosaccharides: production, analysis and*
749 *bioactivity*. New Jersey: Wiley-Blackwell, (Chapter 1).
750 Murthy, K. N. C., Jayaprakasha, G. K., Kumar, V., Rathore, K. S., & Patil, B. S. (2011).
751 Citrus limonin and its glucoside inhibit colon adenocarcinoma cell proliferation
752 through apoptosis. *Journal of Agricultural and Food Chemistry, 59*(6), 2314-2323.
753 Nangia-Makker, P., Hogan, V., Honjo, Y., Baccarini, S., Tait, L., Bresalier, R., & Raz, A.
754 (2002). Inhibition of human cancer cell growth and metastasis in nude mice by oral
755 intake of modified citrus pectin. *Journal of the National Cancer Institute, 94*(24),
756 1854-1862.
757 Ramos-Aguilar, O. P., Ornelas-Paz, J. D., Ruiz-Cruz, S., Zamudio-Flores, P. B.,
758 Cervantes-Paz, B., Gardea-Bejar, A. A., Perez-Martinez, J. D., Ibarra-Junquera, V.,
759 & Reyes-Hernandez, J. (2015). Effect of ripening and heat processing on the
760 physicochemical and rheological properties of pepper pectins. *Carbohydrate*
761 *Polymers, 115*, 112-121.
762 Sathisha, U. V., Jayaram, S., Nayaka, M. A. H., & Dharmesh, S. M. (2007). Inhibition of
763 galectin-3 mediated cellular interactions by pectic polysaccharides from dietary
764 sources. *Glycoconjugate Journal, 24*(8), 497-507.
765 Matsumoto, T., Moriya, M., Sakurai, M. H., Kiyohara, H., Tabuchi, H., & Yamada, H.
766 (2008). Stimulatory effect of a pectic polysaccharide from a medicinal herb, the
767 roots of *Bupleurum falcatum L.*, on G-CSF secretion from intestinal epithelial cells.
768 *International Immunopharmacology, 8*, 581-588.
769 Matsumoto, T., Guo, Y. J., Ikejima, T., & Yamada, H. (2003). Induction of cell cycle
770 regulatory proteins by murine B cell proliferating pectic polysaccharide from the
771 roots of *Bupleurum falcatum L. Immunology Letters, 89*, 111-118.
772 Uchiyama, H., Dobashi, Y., Ohkouchi, K., & Nagasawa, K. (1990). Chemical-change
773 involved in the oxidative reductive depolymerization of hyaluronic-acid. *Journal of*
774 *Biological Chemistry, 265*(14), 7753-7759.
775 Verma, P., Baldrian, P., & Nerud, F. (2003). Decolorization of structurally different
776 synthetic dyes using cobalt(II)/ascorbic acid/hydrogen peroxide system.
777 *Chemosphere, 50*(8), 975-979.
778 Wu, D., Cao, Y. M., Chen, J. C., Gao, H. F., Ye, X. Q., Liu, D. H., & Chen, S. G. (2016).
779 Feasibility study on water reclamation from the sorting/grading operation in
780 mandarin orange canning production. *Journal of Cleaner Production, 113*,
781 224-230.
782 Wu, N., Ye, X. Q., Guo, X., Liao, N. B., Yin, X. Z., Hu, Y. Q., Sun, Y. J., Liu, D. H., &
783 Chen, S. G. (2013). Depolymerization of fucosylated chondroitin sulfate from sea

784 cucumber, Pearsonothuria graeffei, via Co^{60} irradiation. *Carbohydrate Polymers, 93*(2), 604-614.
786 Yan, J. K., Pei, J. J., Ma, H. L., & Wang, Z. B. (2015). Effects of ultrasound on molecular properties, structure, chain conformation and degradation kinetics of carboxylic curdlan. *Carbohydrate Polymers, 121*, 64-70.
789 Yue, W., Yao, P. J., Wei, Y. N., Li, S. Q., Lai, F., & Liu, X. M. (2008). An innovative method for preparation of acid-free-water-soluble low-molecular-weight chitosan (AFWSLMWC). *Food Chemistry, 108*(3), 1082-1087.
792 Sun, Y. J., Ma, G. P., Ye, X. Q., Kakuda, Y., & Meng, R. F. (2010). Stability of all-trans-b-carotene under ultrasound treatment in a model system: Effects of different factors, kinetics and newly formed compounds. *Ultrasonics Sonochemistry, 17*, 654-661.
796 Zhang, L. F., Ye, X. Q., Ding, T., Sun, X. Y., Xu, Y. T., & Liu, D. H. (2013). Ultrasound effects on the degradation kinetics, structure and rheological properties of apple pectin. *Ultrasonics Sonochemistry, 20*(1), 222-231.
799 Zhang, L. F., Ye, X. Q., Xue, S. J., Zhang, X. Z., Liu, D. H., Meng, R. F., & Chen, S. G. (2013). Effect of high-intensity ultrasound on the physicochemical properties and nanostructure of citrus pectin. *Journal of the Science of Food and Agriculture, 93*(8), 2028-2036.
803 Zhi, Z. J., Chen, J. L., Li, S., Wang, W. J., Huang, R., Liu, D. H., Ding, T., Linhardt, R. J., Chen, S. G., & Ye, X. Q. (2017). Fast preparation of RG-I enriched ultra-low molecular weight pectin by an ultrasound accelerated Fenton process. *Scientific Reports, 7*, 1-11.
807
808

Highlights

1. Ultrasonically accelerated metal-free Fenton system was optimized.
2. The mechanism of ultrasound accelerating H_2O_2/ascorbic acid system was clarified.
3. The structure characterization of the resulting fragment (LMP) was determined.
4. The molecular size of pectic polysaccharide is important for its antitumor activity